

ELECTRONIC SUPPLEMENTARY INFORMATION

The Heterogeneous Diffusion of Polystyrene Nanoparticles and the Effect on the Expression of Quorum-Sensing Genes and EPS Production as a Function of Particle Charge and Biofilm Age.

Joann M. Rodríguez-Suárez^{1*}, Anne Gershenson², Timothy Umma Onuh³, Caitlyn S. Butler^{1*}

¹Department of Civil and Environmental Engineering, University of Massachusetts Amherst, Amherst MA 01003

²Department of Biochemistry and Molecular Biology, University of Massachusetts Amherst, Amherst MA 01003

³Department of Chemical Engineering, University of Massachusetts Amherst, Amherst MA 01003

*Correspondence: Caitlyn S. Butler and Joann M. Rodríguez-Suárez

E-mail: csbutler@engin.umass.edu and joan.rodriguez8@upr.edu

Number of pages: 9

Number of figures: 6

Two-dimensional pair correlation function (2D-pCF) and diffusion anisotropy:

The 2D-pCF analysis detects the particle at two different arbitrary but adjacent locations and measures the time it takes for the particle to move from one location to the other. This method allows us to detect barriers to diffusion based on the time it takes for the particle to be detected at the second location. If the time elapsed is longer than the expected average time, the 2D-pCF analysis implies that there is at least one barrier between those two locations (1).

The anisotropy of diffusion, describing the directional dependence of NP diffusion, is obtained from the long and short axes of the 2D-pCF (Fig. S1). The pair correlation function is defined by Equation S1(2):

$$pCF = G(\tau, r_0, r_1) = \frac{\langle F(t, r_0) \cdot F(t + \tau, r_1) \rangle}{\langle F(t, r_0) \cdot F(t, r_1) \rangle} - 1 \quad (\text{S1})$$

where, τ is the time delay between acquisitions of F , the fluorescence intensity at points r_0 and r_1 . The brackets indicate the temporal average. For a given point, r_0 , the pair correlation is measured for points surrounding r_0 that are a given distance δr away. If motion is isotropic, the pCF does not depend on the angle between points r_0 and r_1 and all the pCF curves have the same shape. If motion is anisotropic, for example, if there is a barrier to diffusion in one direction, it will take longer to diffuse the same distance in one direction than in another and the pCF curves will be angle dependent. The angular dependence of the pCF results can be used to calculate anisotropy by Equation S2(1).

$$Anisotropy = \frac{\lambda_1 - \lambda_2}{\lambda_1 + \lambda_2} \quad (\text{S2})$$

where, λ_1 is the long axis where the motion is relatively unhindered and λ_2 is the short axis where motion is hindered. Figure S1 shows a diagram of the anisotropy definition.

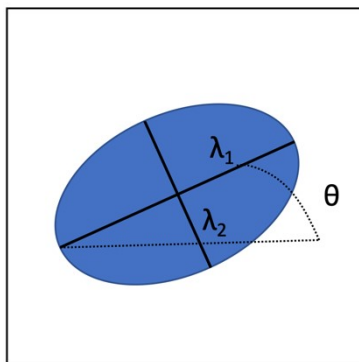


Figure S1 Anisotropy of diffusion definition diagram (Adapted from Malacrida et al. 2018)(1).

Image Mean Square Displacement (iMSD) and diffusion modes:

iMSD is an extension of the spatiotemporal image correlation spectroscopy (STICS) function and can be related to diffusion modes (Figure S2). The modes of diffusion are described by Equation S3(3):

$$\sigma^2(\tau) = \sigma_0^2 + 4D\tau + \frac{L^2}{3}(1 - e^{-k_{micro}\tau}) \quad (S3)$$

where σ^2 is the y-intercept of the MSD versus time curve and is related to the size of the particle, L is the confinement size, k_{micro} is the rate constant for confinement and D is the diffusion coefficient of the particle in the material under study.

The iMSD analysis considers three diffusion modes. These diffusion modes describe particles that are linearly diffusing, confined, or partially confined (Fig. S2)(4). The iMSD method was used to identify and visualize the spatial distribution of diffusion modes and the diffusion coefficients (D) of NPs moving in the biofilms.

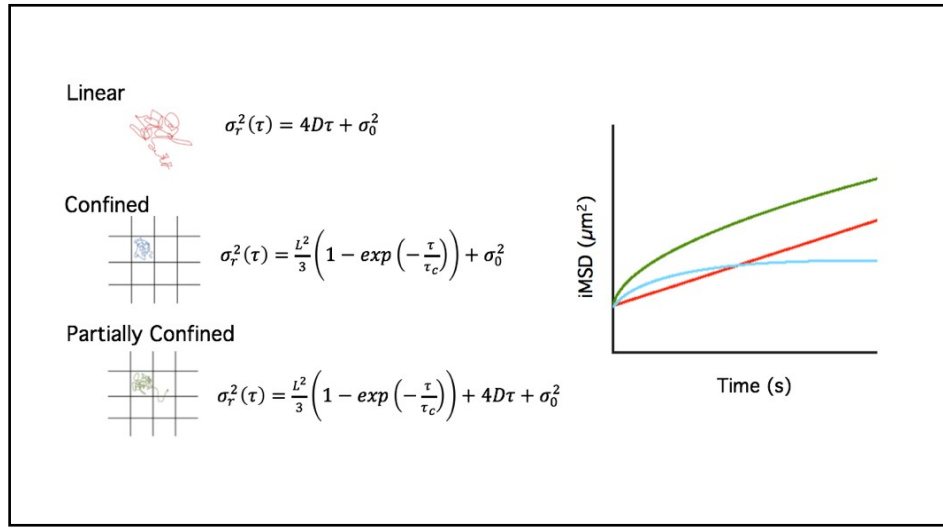


Figure S2 Diffusion modes considered in the iMSD analysis. The iMSD curve shows a linear increase versus time for linear or isotropic diffusion (red curve). The higher the D value the higher the slope which means that the particle moved faster and was able to travel a larger distance in a specific time. For the confined mode of diffusion, the iMSD curve reaches a plateau in a short time indicating that the MSD of the particle does not change with time (blue curve). When particles are confined but find a way to get out of confinement and start moving freely, the iMSD curve starts with a lower slope, but when the particle escapes confinement, the slope suddenly increases (green curve). (Adapted from Moens *et al.* 2015) (4)

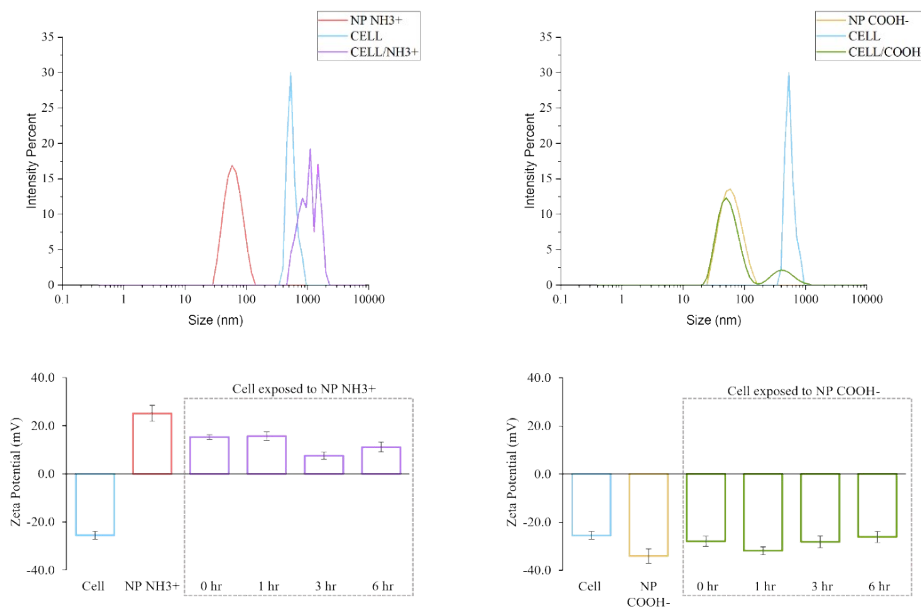


Figure S3: Dynamic light scattering (DLS) Malvern Zetasizer NS (Worcestershire, U.K.) was used to measure the zeta potential and hydrodynamic diameter of the *P. aeruginosa* cells and the NPs individually and in NP-cells samples. In 1 mM HEPES at 37° C, PAO1 $\Delta wspF \Delta psl PBADpel$ cells, the aminated polystyrene NPs and the carboxylated polystyrene NPs have zeta potential of -26 ± 1.7 mV, $+25 \pm 3.3$ mV and -34 ± 3.1 mV respectively. The average size of the cells increased from 515 ± 147 nm to $1,113 \pm 376$ when exposed to the aminated polystyrene NPs which is likely a result of NP attachment to the cell wall.

Microscopy images:

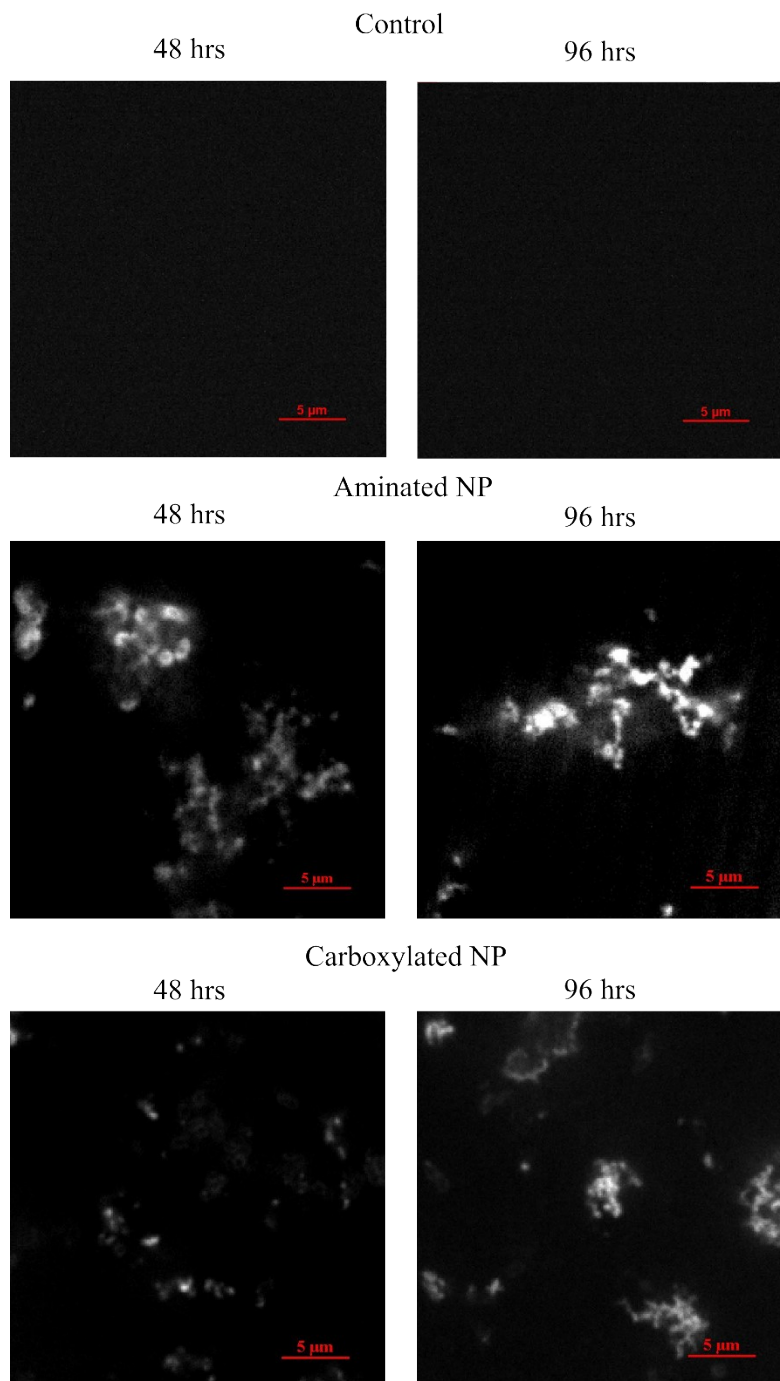


Figure S4: Microscopy images from one field of view for each condition considered in this study. The fluorescent areas (white areas) are the aminated and carboxylated nanoparticles excited with a 561 nm laser. A control sample, a biofilm without nanoparticles, (top) was observed to identify possible background fluorescence emitted from the biofilm components. The scale bar (red) in each image is 5 μm and the images were recorded at a depth of $z = 4500 \pm 703$ μm.

Experiment 2 Results:

Analyses were performed for two independent biofilm samples and analyzed to evaluate the reproducibility of the obtained results. The results are presented in Figures S4, S5 and S6.

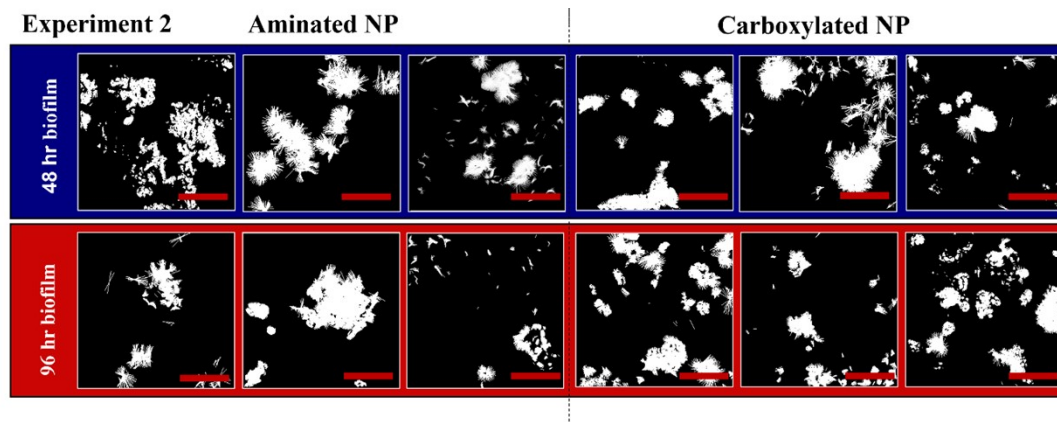


Figure S5: Connectivity maps for all three fields of view ($28.2 \mu\text{m} \times 28.2 \mu\text{m}$) obtained by 2D-pCF analysis for the aminated and carboxylated NPs at a depth of $z = 4500 \pm 703 \mu\text{m}$ for the samples for Experiment 2. Each row shows a field of view analyzed for the 48 hr biofilm samples (blue) and the 96 hr biofilms sample (red). The scale bar (red) in each map is $10 \mu\text{m}$. Anisotropy determined from iMSD analysis for each condition carboxylated is 0.12 ± 0.08 for 48 hours and 0.09 ± 0.01 for 96 hr and aminated NPs is 0.07 ± 0.07 for 48 hours and 0.08 ± 0.04 for 96 hr.

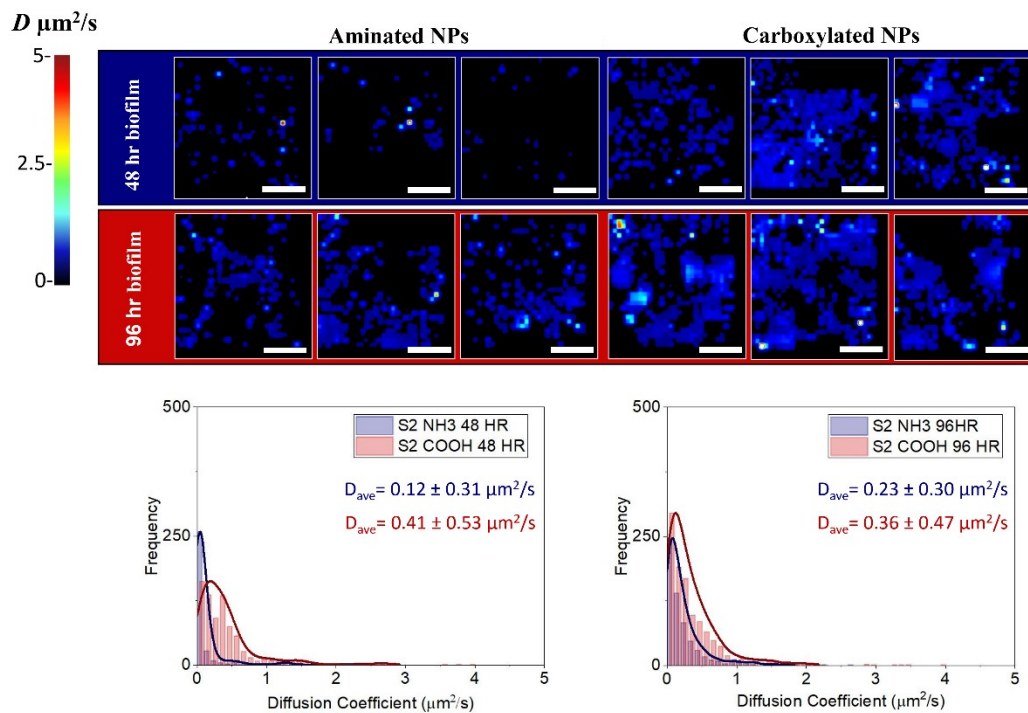


Figure S6: Visual maps and diffusion coefficient histograms for the aminated and carboxylated polystyrene nanoparticles at diffusing at a depth of $z = 4500 \pm 703 \mu\text{m}$. The diffusion coefficients were obtained from the iMSD analysis of images from Experiment 2. The bars are histograms with bins sizes of $0.1 \mu\text{m}^2/\text{s}$. The lines are kernel (Scott) probability density estimates of the diffusion coefficient (D) distributions. Each row shows the maps from the 48 hr and 96 hr biofilm samples. The D heatmap color scale goes from black to red. The red areas are the areas with higher D values and the blacker areas are the ones with the lower D values. The color-coded values in the distribution graphs are average value of the D distributions taking into consideration all 3 fields of view analyzed. The scale bar (white) in each map is $10 \mu\text{m}$.

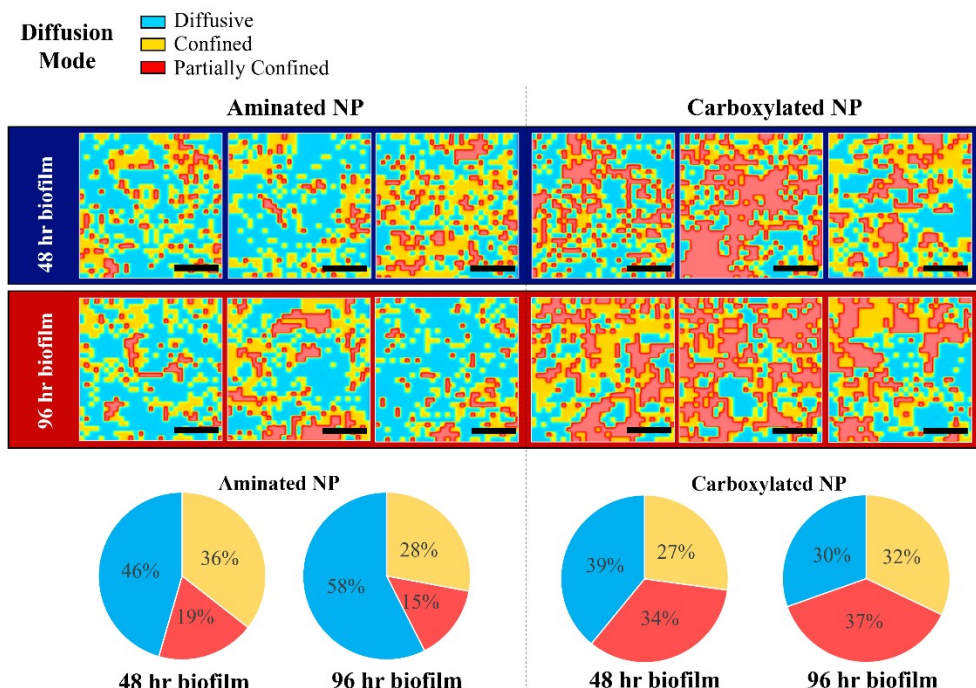


Figure S7: Maps of the distribution of diffusion modes, freely diffusive (blue), confined (yellow) and partially confined (red). Each row shows a field of view analyzed for the 48 hr biofilm and the 96 hr biofilmsamples in Experiment 2. The pie charts represent the average percentage (of the three field of views analyzed) of free diffusion (blue), confined (yellow) or partially confined (red) areas for each type of NP considered. The scale bar (black) in each map is 10 μm and the z depth was $4500 \pm 703 \mu\text{m}$.

REFERENCES

1. Malacrida L, Rao E, Gratton E. Comparison between iMSD and 2D-pCF analysis for molecular motion studies on in vivo cells: The case of the epidermal growth factor receptor. *Methods* [Internet]. 2018 May [cited 2023 Feb 27];140–141:74–84. Available from: <https://linkinghub.elsevier.com/retrieve/pii/S1046202317303614>
2. Digman MA, Gratton E. Imaging Barriers to Diffusion by Pair Correlation Functions. *Biophys J* [Internet]. 2009 Jul [cited 2023 Mar 9];97(2):665–73. Available from: <https://linkinghub.elsevier.com/retrieve/pii/S0006349509009564>
3. Malacrida L, Hedde PN, Ranjit S, Cardarelli F, Gratton E. Visualization of barriers and obstacles to molecular diffusion in live cells by spatial pair-cross-correlation in two

dimensions. *Biomed Opt Express* [Internet]. 2018 Jan 1 [cited 2023 Mar 9];9(1):303. Available from: <https://opg.optica.org/abstract.cfm?URI=boe-9-1-303>

4. Moens PDJ, Digman MA, Gratton E. Modes of Diffusion of Cholera Toxin Bound to GM1 on Live Cell Membrane by Image Mean Square Displacement Analysis. *Biophys J* [Internet]. 2015 Mar [cited 2023 Mar 9];108(6):1448–58. Available from: <https://linkinghub.elsevier.com/retrieve/pii/S0006349515001551>